Analysis of Combustion Hazards due to Catastrophic Failures in Lithium-Ion Battery Packs

Colella, F.*, Marr, K., Ponchaut, N.F., Somandepalli, S., and Spray, R.

Exponent, Inc., Natick, MA, USA.
**Corresponding author email: fcolella@exponent.com*

ABSTRACT

The failure modes of lithium-ion cells have been extensively studied for consumer product applications where the total energy of the battery system is typically below 100 Wh. As lithium-ion cells and systems become larger and more ubiquitous in their use in energy storage, automotive and other vehicular applications, some failure modes that were rare or non-existent in smaller systems are becoming more common. One potentially hazardous failure mode seen in large lithium-ion systems occurs when flammable gases are emitted from a lithium-ion cell, reach the lower explosion limit in a confined space within the chassis of a vehicle, and are ignited by electrical activity or by the cells themselves. If this scenario occurs, the battery containment and the vehicle can become over-pressurized, potentially resulting in an explosion that may cause damage to the vehicle, or its surrounding area, and may result in severe injuries to the vehicle occupants. The research to date has improved the safety of large battery packs but it lacks specific focus on the potential for fires and explosions resulting from cells and batteries going into thermal runaway conditions. In this work, we outline a methodology for quantifying the combustion hazards that can result from cell and battery thermal failures. We have built an apparatus that allows the capture and characterization of the gases released from lithium-ion cells during a thermal runaway failure event. The composition of the gases, their rate of release, their temperature and the total volume of gases released during a thermal runaway event are measured and quantified as a function of cell state of charge and electrode chemistry. Using this experimental data, the distribution of released gas around a failed battery was simulated using Computational Fluid Dynamics (CFD) in two different failure scenarios. The rapid expansion and dispersion of the flammable gas cloud in an open environment and within the battery pack was estimated. Finally, the total amount of flammable gases released as a result of the venting into the surroundings is analysed and quantified.

KEYWORDS: Lithium-ion batteries, overpressure analysis, venting, CFD model.

INTRODUCTION

Rechargeable batteries are ubiquitous in today's electronics, automotive, aerospace, and power storage industries. From smart phones to electric cars, the demand for higher capacity batteries in these applications has been increasing. Lithium-ion (Li-ion) has become the dominant rechargeable cell chemistry for consumer electronics devices and is poised to become commonplace for industrial, transportation, and power-storage applications. This chemistry is different from previously popular rechargeable battery chemistries (e.g., nickel metal hydride, nickel cadmium, and lead-acid) in a number of ways. From a technological standpoint, because of its high energy density, Li-ion technology has enabled entire families of new and smaller devices such as smart phones, electric vehicles etc. From a safety and fire protection standpoint, a high energy density coupled with a flammable organic, rather than aqueous, electrolyte has created a number of new challenges with regard to the design of batteries containing Li-ion cells, and with regard to the storage and handling of these batteries.

There have been numerous fire and explosion incidents associated with Li-ion batteries, ranging from consumer electronic devices such as cellular phones [1] and laptops [2]. Thermal hazards from Li-ion battery failures can be the result of various failure modes. The Li-ion cell chemistry has an

Proc. of the Seventh International Seminar on Fire & Explosion Hazards (ISFEH7), pp. 575–584
Edited by D. Bradley, G. Makhviladze, V. Molkov, P. Sunderland, and F. Tamanini

ISBN: 978-981-07-5936-0 :: doi: 10.3850/978-981-07-5936-0_09-02
www.rpsonline.com.sg

inherent high energy density, and a cell failure can generate significant amounts of heat capable of combusting other cell components. Another hazard can result from a breach in the cell packaging (before or after a thermal event), which can allow for flammable electrolyte vapours to permeate and fill the space where the cells reside, creating a possible explosion risk. Additionally, the degradation and reaction products of a thermal event in a lithium-ion cell and a battery pack can create potentially combustible gases [3] that could create similar explosion risks to that of the un-combusted flammable electrolyte. For large power packs used in electric vehicles and power-storage units, the volume of vented gases may be significant and could pose explosion hazards. Owing to the variability of lithium-ion cell chemical composition due to proprietary manufacture design, the potential explosion severity of the vented gases is not well documented or characterized.

In the present work, the combustion characteristics of vent gases produced due to thermal failure of lithium-ion cells are studied jointly using experiments and Computational Fluid Dynamics (CFD). The goal of the work is to develop a joint experimental and computational methodology to assess potential safety hazards associated with the venting of lithium-ion cells and packs during thermal runaway events. The gases vented from small format lithium-ion cells during thermal runaway are sampled and analysed experimentally. The measured vent gas composition and total volumetric production are then used as input parameters to model two different release events: (1) a release from a single battery in an open environment; (2) a release from a single battery located in the case of a lithium-ion battery pack.

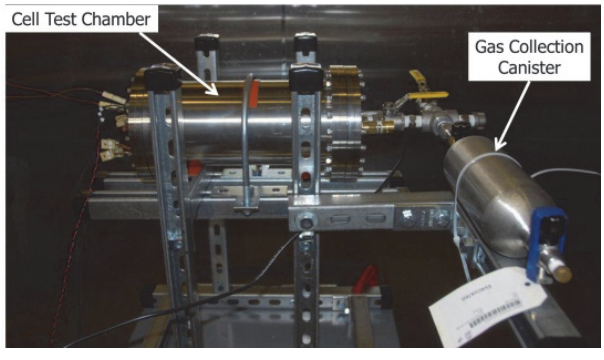

Figure 1. Photograph of battery vent chamber with sample gas canister attached.

EXPERIMENTAL SETUP AND PROCEDURE

Vent products resulting from thermal failure of commercially available 2.1 Ah (7.7 Wh nominal) lithium-ion cells were captured in a custom designed 0.152 m diameter cylindrical stainless steel chamber (see Fig. 1). The cells consisted of a negative electrode with graphite active material and a positive electrode with $LiCoO_2$ active material. The chamber test section is approximately 0.33 m long and is enclosed on either side with 12.7 mm thick stainless steel flanges. On one flange, K-type thermocouples, signal wire pairs to measure battery voltage, and a high voltage power feed thru ports allow for temperature and voltage measurements and power access inside the chamber to monitor the cell health. A pressure transducer, a 3.4 bar pressure relief valve and a gas sampling and vent port were installed on the other flange to monitor and capture the gases released when these cells were made to fail with thermal runaway conditions. For the lithium-ion cell venting experiments, the battery surface temperature, the chamber gas temperature, and the chamber pressure were monitored throughout the duration of each test. Prior to each test, a cell was wrapped with a 100 W, 4.1 mm thick heat cable and placed on a thermal brick inside the vent chamber. The vent chamber was sealed, evacuated with a vacuum pump to approximately 0.04 bar, and refilled

with argon to atmospheric pressure. The purging process with argon was repeated 3 times before each test. Catastrophic failure and subsequent thermal runaway of lithium-ion cells at 50%, 100%, and 150% state-of-charge (SOC) was induced by applying heat to the cell through the heat cable. Power to the heat cable was terminated once the cell failed and gaseous products vented, and the resultant vent products were allowed to collect in the chamber. The gaseous products were allowed to cool to 60°C and were then sampled through the vent port into an evacuated sample canister. The species composition of the gas sample was analysed using gas chromatography-mass spectroscopy (GC-MS). Prior to analysis, the collected gas samples were heated to 60°C to volatilize any gases that may have condensed in the container after the sampling was completed.

EXPERIMENTAL RESULTS

The chamber gas temperature, chamber pressure, battery surface temperature, and cell voltage was monitored throughout the experiment. The experimental data showed that when the battery surface temperature reached approximately 250°C, the cell voltage dropped to zero indicating that the cell had shorted. Immediately following the decrease in voltage, the pressure and temperature of the chamber increased dramatically indicating that the cell had failed and gas had vented. Figure 2 shows an example time trace of chamber pressure, chamber temperature and cell voltage during the 100% SOC test. The total amount of gas produced is estimated from the peak values of the chamber temperature and chamber pressure.

At standard pressure and temperature (300 K, 1 atm), 2.5 l and 6.0 l of gases, respectively, are released from the failure of cells at 100% SOC and 150% SOC. The 150% SOC cell vents more than twice the volume of gas than the 100% SOC cell. As SOC increases, the available potential energy in the cell increases. As a result, more energy is available for phase transitions of the electrolyte and active materials, and therefore a larger volume of gases are vented. The relationship between SOC and vent gas volume is likely nonlinear. However, further investigation is needed to fully characterize this nonlinearity.

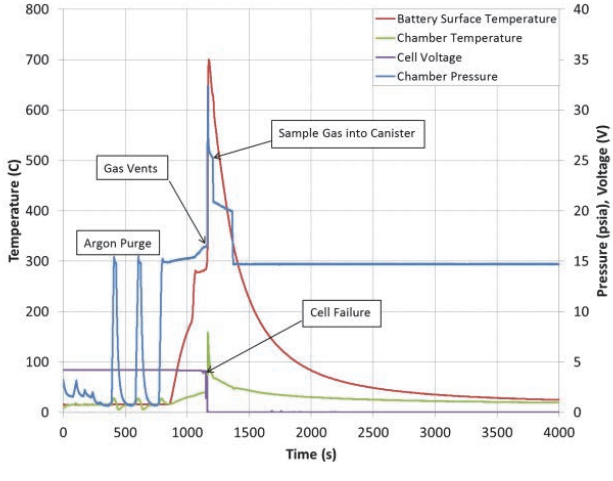

Figure 2. Time trace of cell voltage, chamber pressure, chamber temperature, and battery surface temperature during testing of lithium-ion cells at 100% state-of-charge.

The results of the GC-MS analysis of the sampled gases are summarized in Table 1 for the three states of charge tested. The volume fraction of each species has been adjusted to represent the vent

gases alone by excluding the initial argon and trace oxygen and nitrogen in the chamber. Although the batteries were vented into an inert environment, combustion can still take place due to the decomposition of the positive active material, which produces oxygen. The amount of oxygen produced by the battery is small and is not likely to be sufficient for the fuel to be consumed completely. In all cases tested, significant amounts of hydrogen, hydrocarbons and carbon monoxide were released from the cell. The hydrogen and methane volume fractions were approximately 7% and 28% larger for the 150% SOC compared to the 100% SOC cell. For all the tests, the methane and hydrogen volume fractions are within the flammable limits for their respective species. However, the flammability limits are sensitive the relative amounts of reactive and inert vent products. The ratio of flammable gases, in particular hydrogen, to carbon dioxide directly affects the flammability limits—a larger ratio will widen the flammability range, while a smaller ratio will decrease the flammability range. Depending on cell composition, SOC and other cell characteristics, the vent gas composition, and thus the vent gas flammability limits, may vary significantly. Note that the species volume fractions summarized in Table 1 is for the vent gas that has not yet mixed with air. For any venting event, the region of flammable gas will be dependent on the mixing associated with the release. The fluid mechanics of the venting event is likely dependent on several parameters including SOC, cell composition, battery packaging type, battery pack design, etc.

Table 1. Vent gas species composition for lithium-ion cells at 50%, 100% and 150% state-of-charge.

	50% SOC (%vol)	100% SOC (%vol)	150% SOC (%vol)
Carbon Dioxide	32.3	30.0	20.9
Carbon Monoxide	3.61	22.9	24.5
Hydrogen	31.0	27.7	29.7
Methane	5.78	6.39	8.21
Ethylene	5.57	2.19	10.8
Ethane	2.75	1.16	1.32
Propylene	8.16	4.52	0.013
Propane	0.68	0.26	2.54
Isobutane	0.41	0.20	0.13
n-Butane	0.67	0.56	0.39
Butenes	2.55	1.58	0.60
Isopentane	0.45	0.07	0.036
n-Pentane	1.94	0.73	0.30
Hexanes +	4.94	2.32	0.68
Benzene	0.14	0.11	0.33
Toluene	0.061	0.018	0.052
Ethyl-benzene	0.009	0.002	0.003

Previous studies have reported that the majority of the gas released from a thermally failed lithium-ion cell is carbon dioxide [6,7]. Table 2 compares the volume fraction of the major gas species (CO, CO_2, H_2, CH_4) measured in the present study with the measurements by Roth, et al. [7]. Roth and co-workers vented Li-ion batteries into an inert argon/helium environment and found that, in comparison to the present study, the vent gas composition consists of significantly less hydrogen and carbon monoxide, and significantly more carbon dioxide. It is possible that the differences in results are due to difference in cell composition and cell geometry. The experimental methodologies are also quite different. Roth et al. heated their cells using an Accelerating Rate Calorimeter (ARC)

up to 160°C, which most closely simulates thermal exposure at moderately high temperatures over long periods of time. Because the chemical time scale is potentially long in such an exposure, the chemical reaction is likely to be more complete, which would result in a large volume fraction of carbon dioxide and minimal carbon monoxide.

Table 2. Comparison of vent gas species volume fractions to previous work.

	50% SOC (%vol)	100% SOC (%vol)	150% SOC (%vol)	*Roth et al. [7] (%vol) Test 1/Test 2
Carbon Dioxide	32.3	30.0	20.9	61.4/75.8
Carbon Monoxide	3.61	22.9	24.5	15.1/6.4
Hydrogen	31.0	27.7	29.7	5.1/5.9
Methane	5.78	6.39	8.21	7.4/1.9

*Data from Roth et al. for two vent test for 100% SOC un-aged cells.

The heating method in the present study is designed to initiate an instantaneous violent thermal runaway event by applying a fast temperature ramp rate (~100°C/min). The large volume fraction of carbon monoxide measured in the current study is evidence that the violent release of vent gases in the current study is likely to have resulted in an incomplete combustion reaction. Therefore, the composition of vent gases due to thermal failure of a lithium-ion cell may be highly sensitive to the thermal failure mode. The failure mode considered in the current study is more representative of field failures in individual cells and packs where the transition to thermal runway resulting from mechanical or thermal damage is fast.

CFD SETUP

The numerical model has been developed to simulate two different venting scenarios for a 100% state of charge battery. The first scenario involves a venting event from a single battery in an open environment. The second scenario includes a venting battery located in a common battery pack case containing 19 batteries in total.

The fluid behavior in the 3D sub-domain was modelled using the classical Reynolds-averaged Navier-Stokes equations (RANS) complemented with the k-ε model for turbulence [4]. The standard k–ε model is not valid for fluid regions characterized by a low Reynolds number, in particular locations close to the walls [4]. In these regions the standard wall functions have been used providing adequate results for high Reynolds flows, and avoiding the need to use very fine meshes to resolve the viscous sub-layer.

The CFD model has been implemented in the commercial finite-volume CFD code Star-CCM+ developed by CD-Adapco [5]. Given the large velocity of the gas vented into the domain (~200 m/s) a coupled solver has been used to address the compressible Navier–Stokes problem. The convective fluxes have been approximated by using a second-order upwind scheme. Temporal discretization uses a second order implicit time integration scheme which has the advantage of being unconditionally stable with respect to the time step size. The time-step size has been varied during the course of the simulations and ranged between 10^{-7} s during the initial moments of the release and 10^{-4} s when quasi-steady state conditions were achieved. The simulations time has been limited to 3 s in accordance with the experimental observations regarding the approximate duration of the gas releasing event.

The battery vented gases are simulated as a constant mass flow rate entering the computational domain through the three venting nozzles located on the battery top (see Fig. 3). The mass flow rate has been determined on the basis of the experimental results described in the previous sections. The

solution of species transport equations allowed for evaluating the spatial concentration of the gases released during the venting event and the extension of the flammable zones. Battery walls were conservatively assumed to be adiabatic thus maximizing the temperature rise on the battery walls.

The venting battery has been simulated as located on the base of a cylindrical computational domain (0.5 m radius and 1.5 m height) for scenario 1. Similar approach has been used for scenario 2 where the entire battery pack was located on the base of the cylindrical computational domain. Given the complex battery layout a polyhedral meshing pattern was used. The mesh included only one-sixth of the battery layout by using opportune symmetry boundary conditions. Once a base mesh was produced, the grid was systematically refined in the vicinity of the nozzle venting area. The size of the mesh ranged between 272 k-cell and 374 k-cells for scenario 1 and scenario 2, respectively. The mesh dimension was progressively varied within the computational domain ranging between about 10^{-4} m in the venting area near field and 10^{-2} m in the far field. Figure 3.a and Figure 3.b display the typical meshing structure across a vertical cross section. It can be seen that a large mesh density was achieved via progressive refinements in the nozzle near field area. Figure 3.c presents the mesh details on the battery top surface and shows the relative position of the three venting nozzles. Figure 3.d presents an overall view of the mesh structure used for the simulation of the battery pack release event. A partial view of the casing is also shown on the left hand side together with two of the six casing venting holes (Ø=3 mm) located on the top side of the battery pack.

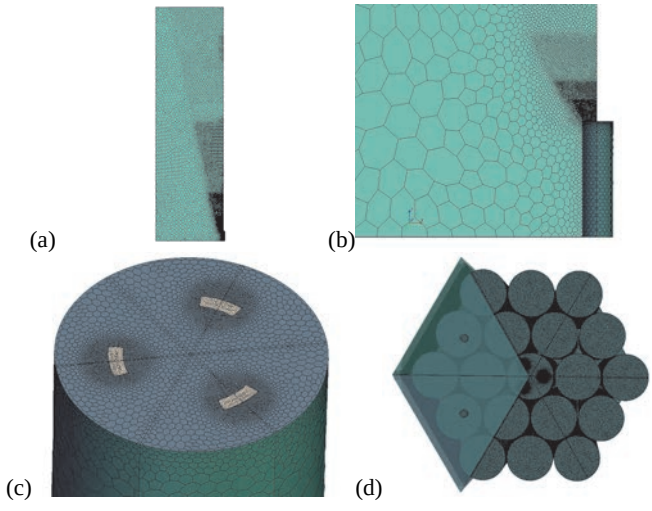

Figure 3. (a) Vertical cross section showing the meshing pattern across the computational domain. (b) Vertical cross section showing the mesh refinements in the proximity of the venting nozzles. (c) Mesh refinements in the nozzle areas. (d) Details of the mesh structure used for the entire battery pack simulation (scenario 2).

CFD RESULTS

This section presents the model predictions, and discusses the main numerical findings. Because of space limitations, temperature and species concentration fields are presented for a limited number of time steps during the venting event.

Figure 4 displays the time dependent evolution of the flammable cloud generated by the venting event previously described as scenario 1 (venting in an open environment). The results are described on a vertical cross sections displaying mole fraction (top) and temperature (bottom) contours. The mole fraction and temperature fields are presented at four different time steps, namely 0.01 s, 0.1 s,

0.5 s and 3 s after the initiation of the release event. The mole fraction contours show a rapid growth of the flammable cloud which reaches its maximum extension between 0.1 s and 0.5 s.

Four continuous black lines are included in the figure representing the 2.5%, 5%, 7.5% and 10% mole fraction iso-contours. The comparison to the venting gas LFL allows evaluating the spatial distribution of the flammable gas regions. This parametric analysis provides additional value due to the large variability associated with the composition of battery venting gases and their corresponding LFL.

The analysis shows that the vertical extension of the flammable gas region ranges between 0.2 m and 0.6 m when the LFL ranges between 10% and 2.5%. The predicted mass of flammable gases is about 0.003 g when the LFL is equal to 10% and 0.04 g if the LFL is equal to 2.5%.

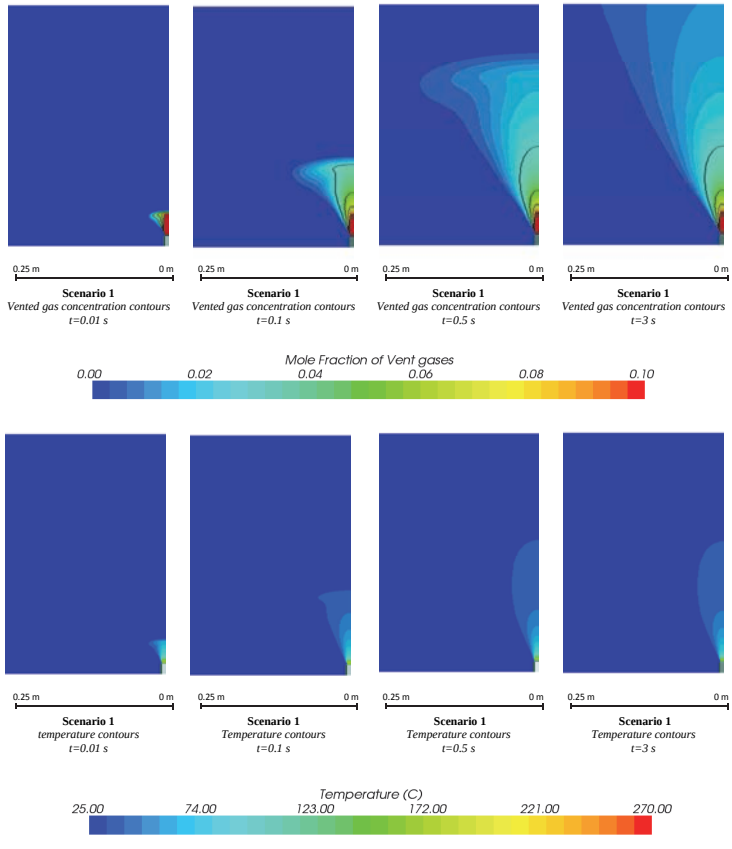

Figure 4. Scenario 1: (top) vertical cross sections showing the venting gas mole fraction contours. The thick black lines correspond to mole fraction iso-contours equal to 2.5%, 5%, 7.5% and 10%; (bottom) vertical cross sections showing the temperature contours. Results are presented for *t=0.01 s, t=0.1 s, t=0.5 s and t=3 s. Not to scale (y-coordinate scaled down by a factor 4).*

Figure 5 displays the time dependent evolution of the flammable cloud generated by the venting event previously described as scenario 2 (venting within the battery pack). Also in this scenario, the mole fraction and temperature fields are presented at four different time steps, namely 0.01 s, 0.1 s, 0.5 s and 3 s after the initiation of the release event. In comparison to scenario 1, the mole fraction contours show a slower growth of the flammable cloud which reaches its maximum extent between

1 s and 1.5 s. This difference with scenario 1 is due to the lower gas velocity through the casing venting holes (Fig. 3.d) than through the battery venting holes (see Fig 3.c).

The analysis shows that the vertical extent of the flammable gas region ranges from 0.2 m to 1.25 m for LFL between 10% and 2.5%. The predicted mass of flammable gases is about 0.08g when the LFL is equal to 10% and 0.5 g if the LFL is equal to 2.5%. In comparison to scenario 1, this scenario is characterized by an increase in the amount of flammable gases released during the venting event by one order of magnitude. This is also the result of poorer fresh air entrainment due to the lower gas velocity through the casing venting holes.

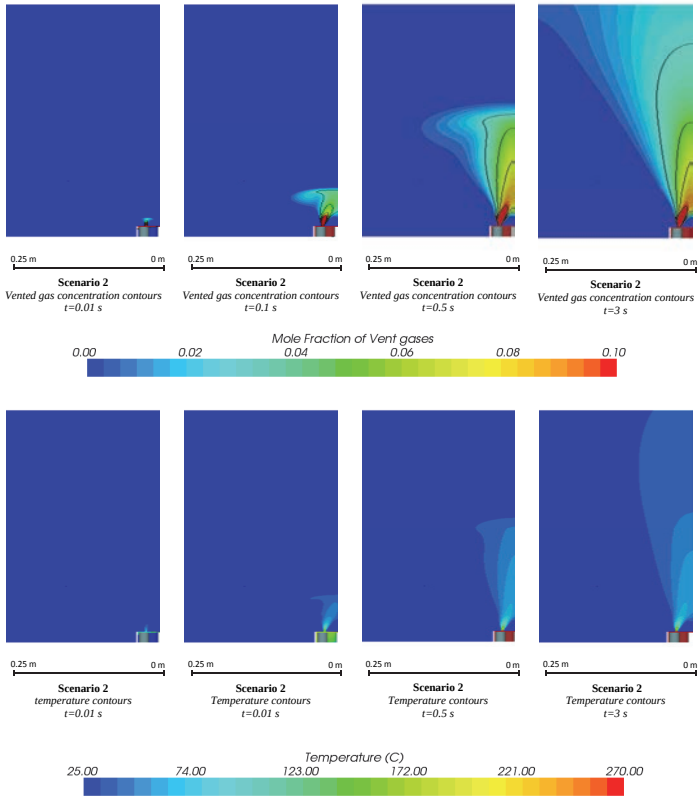

Figure 5. Scenario 2: (top) vertical cross sections showing the venting gas mole fraction contours. The thick black lines correspond to mole fraction iso-contours equal to 2.5%, 5%, 7.5% and 10%; (bottom) vertical cross sections showing the temperature contours. Results are presented for *t=0.01 s, t=0.1 s, t=0.5 s and t=3 s. Not to scale (y-coordinate scaled down by a factor 4).*

Figure 6 shows the mole fraction and temperature contours within the battery pack 0.01 s after the initiation of the release event. The result shows that, within 0.01 s, the entire case volume is filled with flammable gas. In addition, high temperatures are attained which could potentially induce overheating, further shorting and venting of adjacent batteries. CFD results have confirmed that temperatures higher than those presented in Fig. 6, are observed within the battery case at the end of the release event (not shown here).

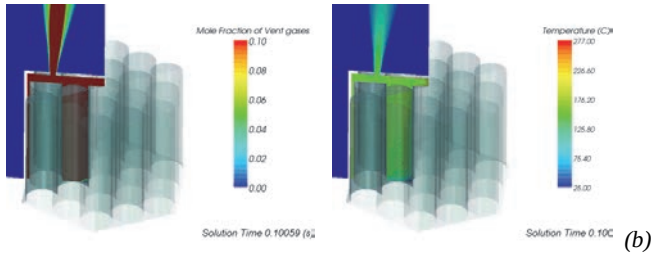

(a) *(b)*

Figure 6. Scenario 2: Vertical cross section showing a detailed view of the temperature *(a)* and venting gas mole fraction *(b)* fields within the battery case for *t=0.01 s*.

CONCLUSIONS

Analysis of combustion hazards due to catastrophic failures of lithium-ion cells has been investigated using a joint experimental and computational methodology. Species composition of the vent gas and total volume of gas vented were determined experimentally. Contrary to previous studies, the vent gas composition was found to contain significant amounts of hydrogen, carbon monoxide and hydrocarbons. The differing results are likely due to both differences in chemical composition of the cell and the methodology of inducing thermal runaway. The vent gas composition and total vent gas volume are also dependent on the state-of-charge of the cell and are likely to be highly sensitive to the specific chemistry of the lithium-ion cell. In addition to state-of-charge and cell composition, cell shape and capacity may also have a large effect on the vent gas characteristics. The results obtained from the experimental investigation have been used in the second portion of the paper to develop a computational model of two venting scenarios: (1) a venting event from a single battery in an open environment and (2) a venting event from a single battery within a battery case. Results show that the CFD analysis is a powerful and compelling technique that allows for a detailed prediction of the flammable regions as well as for an assessment of the amount of flammable gases released. The analysis has also shown the importance of a proper battery venting design.

In particular, for thermal venting event purposes, an optimized design (1) minimizes the adjacent battery overheating to prevent simultaneous shorting and venting and (2) enhances mixing between vented gas and external fresh air in order to confine the spatial extension of flammable gas regions. The methodology presented here has much room for further development. Experimental investigation of a wider range of cell parameters is essential in developing empirical models used to predict vent gas composition and other input variables required for computational modelling. Scaled-up studies for larger format cells used in the automotive, aerospace, and energy storage industries are also needed. Additional work characterizing the heat release rate and other heat transfer characteristics will also aide in understanding the thermal aspects of lithium-ion cell failures. The additional experimental investigations will prompt further computational modelling to identify the correlation between the amount of flammable gas released, the battery capacity (or SOC) and the number of simultaneous venting events. Additional investigation will be necessary to predict the potential overpressure resulting from the ignition of the flammable clouds as well as to identify the key parameters characterizing an optimum battery venting system design.

REFERENCES

1. http://www.cpsc.gov/en/Recalls/2010/Asurion-Recalls-Counterfeit-BlackBerry-branded-Batteries-Due-to-Burn-and-Fire-Hazards/
2. http://www.nytimes.com/2006/08/14/technology/14cnd-battery.html?_r=2&oref=slogin&

3. Harris, S.J., Timmons, A., and Pitz, W.J., "A Combustion Chemistry Analysis of Carbonate Solvents Used in Li-ion Batteries," Journal of Power Sources 193: 855-858 (2009).
4. Versteeg, H.K., and Malalasekera, W., (2007) *An Introduction to Computational Fluid Dynamics, The Finite Volume Method (2nd ed)*, Pearson Prentice Hall, Glasgow.
5. CD-Adapco, Star-CCM+. V 7.04.011
6. Crafts, C., Borek, T., and Mowry. C., "Safety Testing of 18650-Style Lithium-ion Cells," Sandia National Laboratories, SAND2000-1454C, May 2000.
7. Roth, E.P., Crafts, C.C., Doughty, D.H., and McBreen, J., "Advanced Technology Development Program for Lithium-Ion Batteries: Thermal Abuse Performance of 18650 Li-Ion Cells," Sandia Report: SAND2004-0584, March 2004.